Electron-energy-loss spectroscopy of plasmon excitations in concentric-shell fullerenes

Henrard, L.; Malengreau, F.; Rudolf, P.; Hevesi, K.; Caudano, R.; Lambin, Ph.; Cabioc'h, Th.

Published in:
Physical Review B

DOI:
10.1103/PhysRevB.59.5832

Publication date:
1999

Electron-energy-loss spectroscopy of plasmon excitations in concentric-shell fullerenes

L. Henrard,* F. Malengreau,† P. Rudolf, K. Hevesi, R. Caudano, and Ph. Lambin
Département de Physique, Facultés Universitaires Notre-Dame de la Paix, B-5000 Namur, Belgium

Th. Cabioc'h
Laboratoire de Métallurgie Physique, Université de Poitiers, UMR 6630 CNRS, SP2MI, Bd3, Téléport 2, BP 179, 86960 Futuroscope Cedex, France

(Received 9 February 1998; revised manuscript received 2 September 1998)

We report evidence for surface plasmon excitations in concentric-shell fullerenes. A film of these concentric-shell fullerenes with radii around 5–7 nm was produced by carbon bombardment of a silver polycrystalline target and measured by electron-energy-loss spectroscopy (EELS) in reflection geometry. These data were analyzed with the help of a dielectric theory developed for EELS in transmission geometry. Taking into account the concentric-shell–substrate interaction, the spectral shape can be explained as a combination of contributions from σ-π^* interband transitions (around 13.5 eV), from the surface radial (σ-π^*) and tangential (σ-σ^*) plasmons (around 14.5 eV and 16.7 eV, respectively), and from the volume plasmon (24.5 eV). [S0163-1829(99)03107-0]

I. INTRODUCTION

Concentric-shell fullerenes were discovered in the transmission electron microscope under intense electron irradiation of carbon soot.[1] Since that time, other production methods have been developed, such as a thermal treatment of carbon soot[2] and nanodiamonds.[3] Even before any production techniques existed, concentric-shell fullerenes were proposed as possible interstellar dust components.[4] This hypothesis was recently supported by a theoretical investigation of the optical properties of these molecules.[5] Another exciting application of these particles is that they can act as nanoscopic pressure cells, leading to the formation of nanodiamonds in the core of the particles.[6]

Recently, Cabioc'h *et al.* developed a production method based on the bombardment of Cu (Ref. 7) or Ag (Ref. 8) substrates by C ions. The main advantage of this technique over the other methods is its ability to produce films of concentric-shell fullerenes. Up to now, the small quantity of multishell fullerenes produced by all the available techniques has curbed the complete physical characterization of this material. To our knowledge, only optical measurements on poorly formed molecules,[2] transmission electron-energy-loss spectra[8] (T-EELS), and infrared spectroscopy data[9] have been reported in the literature. The synthesis of thin films opens new opportunities to study the physical properties of concentric-shell fullerenes using surface spectroscopy.

In this paper, we report on the first study of the dielectric properties of concentric-shell fullerenes realized by reflection EELS (R-EELS). We performed the EELS measurements on a thin film of fullerenes produced by C-ion implantation in Ag (Ref. 8) (see Sec. II). We analyzed the results in terms of the combined excitation of surface and bulk plasmons, and interband transitions in the carbon particles. Our discussion is supported by a theoretical treatment based on a dielectric model and a discrete dipole approach (see Sec. III).

II. EXPERIMENTAL RESULTS

The formation of concentric-shell fullerenes in a silver substrate was achieved using the ion-implantation technique fully described in Ref. 8. In the present case, a high dose (5×10^{17} cm^{-2}) of 120-keV C_{12}^{+} ions was implanted into a large polycrystalline silver sheet (purity $>99.99\%, 1\times1\times0.2$ cm^3) held at high temperature (773 K). This led to the formation of a high-density layer of carbon particles on the silver surface, or in the near-surface region, as discussed below.

Figure 1(a) shows an atomic force microscopy (AFM) image of the implanted silver surface obtained with a Nanoscope Digital instrument. Numerous concentric-shell fullerenes emerging from the surface can be observed. We also show on Fig. 1(b) a typical high-resolution transmission electron microscopy (HRTEM) micrograph of these concentric-shell fullerenes. The HRTEM experiments have been performed on polycrystalline silver disks (3 mm in diameter) where the areas observed by TEM were obtained by a chemical polishing of the backside of the substrate. We emphasize the remarkable sphericity of the concentric-shell

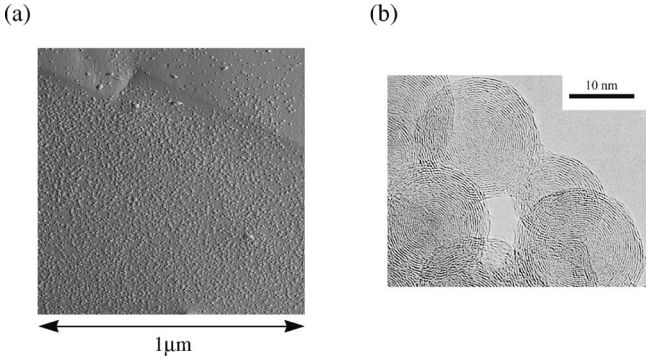

FIG. 1. AFM (a) and TEM (b) images of a concentric-shell fullerene layer produced by carbon-ion implantation into a Ag polycrystal.

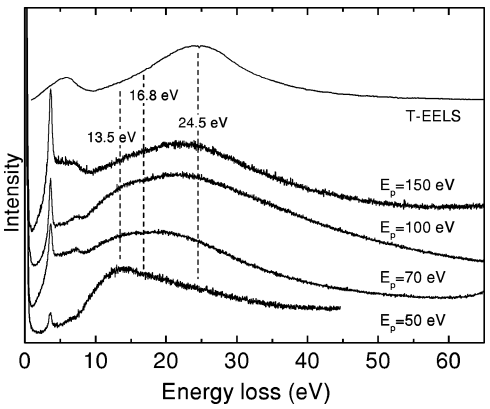

FIG. 2. Electron-energy-loss experimental results. The top curve is a transmission-EELS result given for comparison. The other spectra are reflection-EELS measured on a concentric-shell fullerene layer in the specular geometry with different primary energies (150, 100, 70, and 50 eV from top to bottom). All R-EELS spectra are normalized to the elastic peak intensity and the spectra for $E_p = 150$ eV and $E_p = 50$ eV are plotted with amplification factors of 1.7 and 0.6, respectively.

fullerenes and also their homogeneity in size (5–7 nm radii). It is important to note that (i) the concentric-shell fullerenes are distributed uniformly throughout each crystalline grain of the silver substrate and (ii) a very high density of concentric-shell fullerenes can be achieved. On the AFM image in particular, one observes that the carbon particles are more or less embedded in the bulk of Ag. We explain these observations as follows: implanted carbon atoms precipitate in the bulk of the silver substrate leading to the formation of concentric-shell fullerenes during the implantation process. Since the silver surface is extensively sputtered, wheras the carbon sputtering yield remains very low, the carbon aggregate formed in the bulk finally emerge at the surface. The silver sputtering yield depends on the silver grain orientation, which can explain why the density of the concentric-shell fullerenes as observed by AFM varies from grain to grain.

The reflection energy-loss experiments were performed in an ultrahigh-vacuum (UHV) system equipped with an ISA-Riber SEDRA high-resolution EELS spectrometer and a fast entry lock for sample introduction. The energy of the incident electron beam was varied between 50 and 150 eV and the instrumental resolution was set to 0.1 eV. All the R-EELS measurements presented in this paper were carried out in the specular reflection geometry ($\theta_i = \theta_r = 45°$). The size of the probing beam was about 1 mm^2.

In Fig. 2, electron-energy-loss spectra obtained in the 0–50-eV loss range are displayed for several primary energies (E_p) of the incident electron beam. For comparison we also plot (top curve) a typical T-EELS spectrum obtained on a similar sample[8] (the zero-loss peak has been removed for clarity). The origin of the main loss features can be summarized as follows. The 3.5-eV peak is attributed to the *surface* plasmon of the Ag substrate.[10] The structure between 5 and 7 eV combines both the 5.7-eV Ag *volume* plasmon[10] and the π surface and volume plasmon excitations of the carbon shell, which we were not able to separate in our data. The Ag plasmon does not appear in the T-EELS data because the nonimplanted face of the substrate was chemically etched. As a consequence, the transmission spectrum arises from concentric-shell fullerene excitations only. In R-EELS, the weight of the Ag surface plasmon increases with increasing primary energy because the penetration depth of the electrons becomes larger and the inelastic scattering range changes as the momentum transfer decreases (see Sec. IV).

At higher loss energies, a very broad feature is observed and its maximum is seen to shift to higher loss energies with increasing primary energy. In the Discussion (Sec. IV) we will explain that this feature contains contributions from σ-π^* interband transitions (around 13.5 eV) and from $\sigma + \pi$ plasmons. Among the latter, the surface radial (σ-π^*) plasmon (14.5 eV), the tangential (σ-σ^*) plasmon (around 16.7 eV) and the volume plasmon (25 eV) show up with different weights in spectra taken at different primary energies.

III. THEORETICAL MODELING

In this section, we analyze the results presented above in the light of EELS numerical modeling. We also investigate the role of the Ag substrate on the surface resonance modes of the spherical carbon shells.

In previous works,[11,12] we computed the energy loss of an electron passing near a spherical (concentric-shell) carbon or a cylindrical (cigar-shaped) particle. Two models were developed. The first one was based on the multipole dynamical polarizability $\alpha_l(\omega)$ of a perfectly spherical concentric-shell fullerene.[12] The loss probability $P(\omega)$ was then evaluated through a dielectric model for a classical trajectory.[13]

In the second discrete dipole approximation (DDA) scheme,[11] a hyperfullerene particle was viewed as a set of dipoles $\mathbf{p}_i$ located at the positions $\mathbf{r}_i$ of the atoms. To each carbon was assigned a dipolar tensor of the form[11,14]

$$\vec{\alpha}(\omega) = \alpha_{\parallel}(\omega)\mathbf{rr} + \alpha_{\perp}(\omega)(\theta\theta + \phi\phi), \tag{1}$$

where $\alpha_{\parallel}(\omega)$ and $\alpha_{\perp}(\omega)$ were taken from the graphite dielectric function via a Clausius-Mosotti-like relation.[11,14] The input dielectric tensor was taken from published experimental data.[15] The loss probability $P(\omega)$ was computed for an electron moving on a classical trajectory along oz and interacting with all the dipoles. This led us to

$$P(\omega) = \frac{q\omega}{4\pi^2\epsilon_0 v^2\hbar^2} \sum_i e^{-i\omega z_i/v}\mathbf{a}_i(\omega)\cdot\mathbf{p}_i(\omega) \tag{2}$$

with

$$\mathbf{a}_i(\omega) = (\mathbf{d}_{oi}K_1(\omega d_i/v), -iK_0(\omega d_i/v)), \tag{3}$$

where $\mathbf{d}_i$ is the impact parameter measured from $\mathbf{r}_i$, z_i is the z component of $\mathbf{r}_i$, q is the charge of the electron with velocity v, and K_m is the modified Bessel function of order m.

In Eq. (2), the $\mathbf{p}_i$'s are the dipole moments induced by a Fourier component $\mathbf{E}^e(\omega)$ of the total electric field. A contribution of it is the Coulomb field of the moving electron evaluated at position $\mathbf{r}_i$,

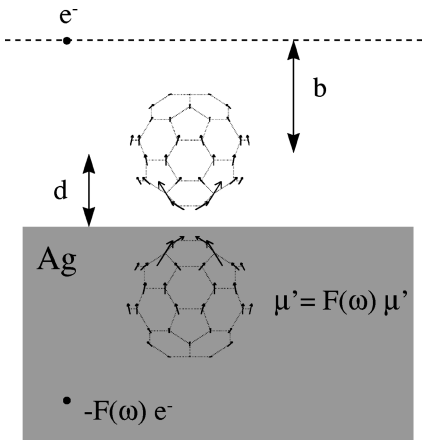

FIG. 3. Schematic representation of an electron passing near a fullerene molecule interacting with the silver substrate via image dipole theory. $F(\omega)=[\epsilon_s(\omega)-1]/[\epsilon_s(\omega)+1]$.

$$\mathbf{E}^e(\omega)=\frac{q\omega}{2\pi\epsilon_0 v^2}\, e^{iwz_i/v}(\mathbf{d}_{oi}K_1(\omega d_i/v),\quad iK_0(\omega d_i/v)). \tag{4}$$

To this field, we need to add the one generated by the other dipoles, and the field induced by the Ag substrate. The latter is evaluated through the image approximation[16] as illustrated in Fig. 3. The atomic dipole moments $\mathbf{p}_i(\omega)$ are then solutions of the set of coupled equations

$$\mathbf{p}_i(\omega)=\overleftrightarrow{\alpha}(\omega)\mathbf{E}_i(\omega),$$

$$\mathbf{E}_i(\omega)=\mathbf{E}^e(\omega)+\sum_{j\neq i=1}^{N}[\overleftrightarrow{T}(\mathbf{r}_i-\mathbf{r}_j)+\overleftrightarrow{T}'(\mathbf{r}_i-\mathbf{r}_{j'})]\mathbf{p}_j(\omega)$$

$$+\overleftrightarrow{T}'(\mathbf{r}_i-\mathbf{r}_{i'})\mathbf{p}_i(\omega),\quad i=1,\ldots,N, \tag{5}$$

where $\mathbf{E}^e(\omega)$ is now the external field generated by the moving electron and by its image charge and where $\overleftrightarrow{T}(\mathbf{r}_i-\mathbf{r}_j)$ denotes the dipolar tensor; $\overleftrightarrow{T}'(\mathbf{r}_i-\mathbf{r}_{j'})=\overleftrightarrow{S}\overleftrightarrow{T}(\mathbf{r}_i-\mathbf{r}_{j'})$ with $\mathbf{r}_{j'}$ being the position of the image dipole relative to the substrate surface $(z=0)$, and

$$\overleftrightarrow{S}=\frac{\epsilon_s(\omega)-1}{\epsilon_s(\omega)+1}\begin{pmatrix}-1 & & \\ & -1 & \\ & & 1\end{pmatrix}$$

is the electrostatic field propagator[16] with $\epsilon_s(\omega)$ the dielectric function of the substrate (Ag in the present study[17]).

IV. DISCUSSION

The dielectric model and the classical electron approximation have given satisfactory results for the interpretation of EELS data in both transmission and reflection geometries.[18] Our dipole model for anisotropic concentric-shell fullerenes has already demonstrated its validity for simulating both optical measurements[12,19] and the van der Waals adsorption of C_{60} on a surface.[20] It should therefore be applicable in the present context, although the formulation of Sec. III is only valid for an electron traveling along a straight-line trajectory parallel to the substrate. The calculations presented above are thus better suited to describe spatially resolved T-EELS data than R-EELS experiments. In addition, the model only accounts for long-range inelastic (dipolar, quadrupolar, etc.) scattering. However, since surface excitations are dominant in R-EELS, the model still gives useful predictions.

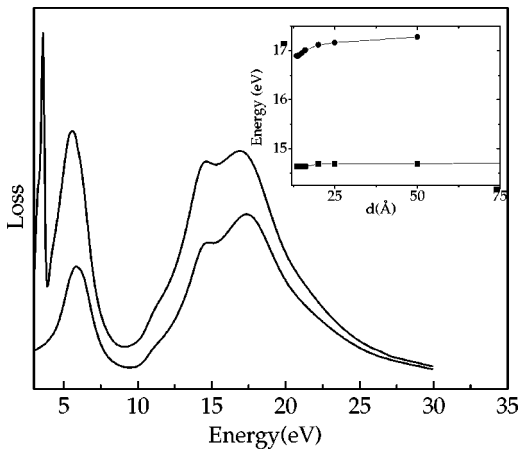

FIG. 4. Simulated electron-energy-loss spectrum for a 100-keV electron passing nearby a $C_{60}@C_{240}@C_{540}$ molecule. The impact parameter is 20 Å . The lower curve is for an isolated molecule and the upper curve is for a molecule lying on an Ag substrate. Inset: Position of the surface $\sigma+\pi$ and σ-π* resonance of a $C_{60}@C_{240}@C_{540}$ molecule as a function of the distance d between the molecule center and the substrate surface.

In transmission geometry, isolated concentric-shell fullerenes are predicted to give a $\sigma+\pi$ volume-plasmon loss centered at 25 eV for a penetrating electron.[11,21] This correlates well with the experimental results presented above and with the measurements of the volume plasmon in carbon nanotubes.[22,23] We also predicted[11] two surface plasmons associated with a tangential (σ-σ*) and a radial (σ-π*) excitation of the carbon anisotropic shell, respectively. These two modes are analogous to the symmetric and antisymmetric modes of a free-standing dielectric film. The more intense tangential mode is found to be between 14.5 and 17.5 eV depending of the size of the internal cavity. For completely filled concentric-shell fullerenes like those produced by ion implantation, it was calculated at 17.5 eV.[11] The radial mode was found to be at 14.8 eV for all concentric-shell fullerenes.

In our experiment the concentric-shell fullerenes are not isolated, so the presence of the substrate has to be taken into account. Figure 4 compares the theoretical EELS spectrum for an isolated $C_{60}@C_{240}@C_{540}$ molecule to the one calculated for the same molecule lying on a Ag substrate. A clear effect of the substrate is to shift the frequency of the surface plasmon modes. There is a small broadening of the modes as well, which is hardly visible when using a realistic dielectric function.

In Fig. 4, the inset presents the shift of the surface plasmon resonance of the $C_{60}@C_{240}@C_{540}$ molecule as a function of the distance d from the molecule center to the surface obtained with the experimental dielectric data.[15] As expected, there is a redshift of the excitation energy as the molecule approaches the surface (the molecular radius is 12 Å). At contact distance,[24] the resonance is reduced to 16.7 eV for the tangential plasmon and 14.5 eV for the radial

mode. The larger shift of the tangential plasmon is explained by the more important coupling of this mode to the substrate due to its larger polarizability. This effect could be experimentally checked if similar experiments were done on a dielectric substrate instead of a metallic one but the production of concentric-shell fullerenes by ion implantation constraints us to metallic substrates.

The next step towards the comprehension of the experimental data consists in taking into account that, as observed in the AFM picture in Fig. 1, the concentric-shell fullerenes are close enough that the presence of neighboring particles can influence the surface plasmon energy. As a first approach to this problem we used the Clausius-Mosotti relation:[25] in our model (Sec. III), we took the dipolar ($l=1$) term and computed the dielectric function of the layer of concentric-shell fullerenes as a function of the onion density. Estimating the average density from Fig. 1 to be 2×10^{-10} Å^{-3}, this leads to a negligible shift of the loss peak compared to the case of an isolated concentric-shell fullerene. Nevertheless, in many points of the sample surface small clusters of several particles are seen and there the local density is substantially higher than the average value mentioned above. For such small clusters the surface plasmon will be redshifted. However, no definitive conclusion can be drawn from this result since higher multipolar order interactions might not be negligible for large molecules such as fullerenes,[26] especially when they form clusters, and the Clausius-Mosotti formula could be not entirely valid, as a consequence.

We now turn to the detailed analysis of the data presented in Fig. 2. From the above analysis of the substrate-concentric-shell interaction on collective excitations, we are not able to explain the dominant intensity of the 13.5-eV peak for $E_p=50$ eV, whereas the radial surface plasmon is expected at 14.5 eV, nor the fact that the predicted 16.7-eV surface plasmon mode does not clearly show up in the experimental data. We have adressed these two questions as follows.

As the local electronic density of states of the concentric-shell fullerenes should not differ much from that of graphite, the loss spectra of these two forms of carbon should show similar features. In graphite, a loss peak is found around 13 eV which is attributed to σ-π^* interband transitions contributing to the out of plane component of the dielectric tensor.[27] For low E_p (50 eV), the momentum transfer accompanying the loss at 13.5 eV is large, of the order of 2.5 Å^{-1}. In these conditions, the inelastic scattering of the incident electrons is short ranged[28] and the interband transitions dominate. The model we presented in Sec. III does not include such short-wavelength excitations of the concentric-shell fullerene molecules because it is based on long-wavelength dielectric data. As E_p increases, the transferred momentum decreases and the range of the interaction becomes larger. As a consequence the radial surface plasmon mode (predicted at 14.5 eV) acquires more intensity. This explains why the higher-energy spectral feature in the $E_p=50$ eV spectrum is peaked at 13.5 eV.

Let us now consider why the radial and the tangential surface plasmons do not show up as separate peaks and why the most intense resonance (tangential mode) in the T-EELS calculation (Fig. 4) is not clearly prominent in the experimental R-EELS. Both theoretical and experimental[29] results in T-EELS show that the position of the resonance associated with the tangential surface plasmon depends on the impact parameter of the incident electron beam. This is due to the variation of different multipolar responses upon change of the impact parameter. On the other hand, a change in impact parameter does not affect the radial surface plasmon energy. It is obvious that the impact parameter is an ill-defined quantity in R-EELS. For our experimental data, we should therefore consider an average over all impact parameters. Consequently, the resonance with an energy dependence on the impact parameter is expected to be very broad and less intense whereas the resonance with no dependence on the impact parameter appears relatively stronger in the spectrum. This explains why we see just one broad structure between 10 and 20 eV instead of separate radial and tangential plasmon peaks.[30]

When the primary energy of electrons E_p increases beyond 70 eV, a resonance centered around 24.5 eV appears. In the T-EELS spectrum, the 24.5-eV broad peak is clearly associated with the bulk plasmon excitation of the concentric-shell fullerenes, since the electron beam penetrates the concentric-shell fullerenes.[8] For tubular carbon particles, a bulk plasmon excitation was found between 20 and 27 eV depending on the internal and external radii of the nanotubes.[22,23] The 24.5-eV peak observed in R-EELS with high primary energy can therefore also be assigned to the bulk plasmon excitation. At lower primary energy, the intensity of the volume plasmon decreases because the penetration depth of the electrons in carbon decreases. This interpretation is supported by the fact that the probing depth of electrons in fullerene is minimum for 50-eV electrons.[31]

In conclusion, we have reported experimental evidence for a surface plasmon excitation in concentric-shell fullerenes. We analyzed these R-EELS data with the help of a dielectric theory developed for T-EELS, by focusing on the existence of two surface plasmon modes (tangential and radial) associated with the anisotropic carbon shell and considering the interaction between the concentric-shell fullerene particles and the Ag substrate. We found that the spectral shape can be explained as due to contributions from σ-π^* interband transitions (around 13.5 eV), from the surface radial (σ-π^*) plasmon (14.5 eV), from the surface tangential (σ-σ^*) plasmon (around 16.7 eV), and the volume plasmon (24.5 eV), which show up with different weights in spectra taken at different primary energies.

Further theoretical investigation is needed for modeling the plasmon excitation in reflection geometry, as well as for understanding the effect on the plasmon energy of both the clustering of the concentric-shell fullerenes, and their partial embedding into the substrate. EELS data for a different size of concentric-shell fullerenes and for concentric-shell fullerenes deposited on various substrates will also be determinant tests for the models.

ACKNOWLEDGMENTS

This work has been performed under the auspices of the Belgian State Interuniversity Research Program on reduced dimensionality systems (PAI/IUAP No 4/10) and has received partial financial support from the ''Actions intégrées franco-belges Tournesol'' (Project No. 98.034).

*Present address: Groupe de Dynamique des Phases Condensées, Université de Montpellier II, Place E. Bataillon CC026, 34095 Montpellier, France. Electronic address: henrard@gdpc.univ-montp2.fr

†Permanent address: Glaceries de Saint-Roch SA, Centre de Developpement, Rue des Glaces Nationales, 169 B-5060 Sambreville, Belgium.

[1] D. Ugarte, Nature (London) **359**, 707 (1992).

[2] W. A. de Heer and D. Ugarte, Chem. Phys. Lett. **207**, 480 (1993).

[3] V. L. Kuznetsov, A. L. Chuvilin, Y. V. Butenko, I. Y. Malkov, and V. L. Titov, Chem. Phys. Lett. **222**, 343 (1994).

[4] H. W. Kroto and K. McKay, Nature (London) **331**, 328 (1988).

[5] L. Henrard, Ph. Lambin, and A. A. Lucas, Astrophys. J. **487**, 719 (1997).

[6] F. Banhart and P. M. Ajayan, Nature (London) **382**, 433 (1996).

[7] T. Cabioc'h, J. P. Riviere, and J. Delafond, J. Mater. Sci. **30**, 4787 (1995).

[8] T. Cabioc'h, J. C. Girard, M. Jaouen, and M. F. Denanot, Europhys. Lett. **38**, 471 (1997).

[9] T. Cabioc'h, A. Kharbach, A. Le Roy, and J. P. Rivière, Chem. Phys. Lett. **285**, 216 (1998).

[10] F. Moresto, M. Rocca, V. Zielasek, T. Hidelbrandt, and M. Henzler, Surf. Sci. **388**, 1 (1997).

[11] L. Henrard and Ph. Lambin, J. Phys. B **29**, 5127 (1996).

[12] A. A. Lucas, L. Henrard, and Ph. Lambin, Phys. Rev. B **49**, 2888 (1994).

[13] P. M. Echenique, A. Howie, and D. J. Wheatley, Philos. Mag. B **56**, 335 (1987).

[14] L. Henrard *et al.*, Fullerene Sci. Technol. **4**, 133 (1996).

[15] B. T. Draine and H. M. Lee, Astrophys. J. **285**, 89 (1984).

[16] G. D. Mahan and A. A. Lucas, J. Chem. Phys. **68**, 1344 (1978).

[17] E. D. Palik, *Handbook of Optical Constants of Solids II* (Academic Press, Boston, 1991).

[18] A. A. Lucas and M. Sunjic, Prog. Surf. Sci. **2**, 75 (1972).

[19] L. Henrard, P. Senet, Ph. Lambin, and A. A. Lucas, Synth. Met. **77**, 27 (1996).

[20] P. A. Gravil, Ph. Lambin, G. Gensterblum, L. Henrard, P. Senet, and A. A. Lucas, Phys. Rev. B **53**, 1622 (1996).

[21] T. Stöckli, J. M. Bonard, A. Châtelain, Z. L. Wang, and P. Stadelman, Phys. Rev. B **57**, 15 599 (1998).

[22] P. M. Ajayan, S. Iijima, and T. Ichihashi, Phys. Rev. B **47**, 6859 (1993).

[23] L. A. Bursill, P. A. Stadelman, J. L. Peng, and S. Prawer, Phys. Rev. B **49**, 2882 (1994).

[24] In our calculation we cannot consider the partial embedding of the concentric-shell fullerenes in the Ag substrate which will also influence the plasmon energy. The EELS spectra of an isotropic dielectric sphere embedded in a dielectric material have already been formulated in N. Zabala and A. Rivacoba, Phys. Rev. B **48**, 14 534 (1993); A. Rivacoba, N. Zabala, and P. M. Echenique, Phys. Rev. Lett. **69**, 3362 (1992); and Z. L. Wang and J. M. Cowley, Ultramicroscopy **21**, 347 (1987), where the authors emphasized the existence of a new mode (an interface mode) at lower energy.

[25] C. Kittel, *Introduction to Solid State Physics*, 5th ed. (Wiley, New York, 1976).

[26] Ph. Lambin, A. A. Lucas, and J. P. Vigneron, Phys. Rev. B **46**, 1794 (1992).

[27] E. Tosatti and F. Bassani, Nuovo Cimento **65**, 161 (1970).

[28] H. Ibach and D. L. Mills, *Electron-Energy-Loss Spectroscopy and Surface Vibrations* (Academic Press, New York, 1982).

[29] O. Stephan, L. Henrard, and C. Colliex (unpublished).

[30] Kinematic effects can also affect the relative intensity of plasmon resonance: as seen in Sec. III, at lower primary energy, the electrons excite low-energy resonances with higher probability. This could also play a role in the observed intensity of the radial mode compared to the tangential one.

[31] A. Goldoni, C. Cepek, and S. Modesti, Synth. Met. **77**, 189 (1996).